Article

Cell

The Cellular Mechanisms of Neuronal Swelling Underlying Cytotoxic Edema

Graphical Abstract

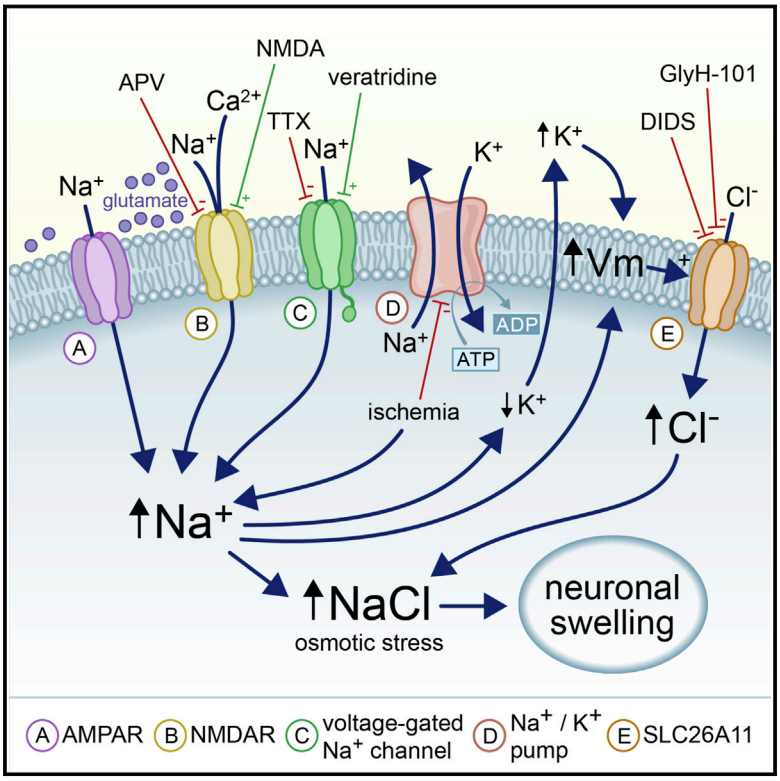

Highlights

- Neuronal swelling depends on Na^+ and Cl^- influx but is independent of Ca^{2+} influx
- Neuronal swelling after Na^+ and Cl^- influx causes Ca^{2+}-independent neuronal death
- Knockdown of the ion exchanger SLC26A11 attenuates neuronal swelling
- SLC26A11-dependent Cl^- influx occurs via voltage-gated Cl^- channel activity

Authors

Ravi L. Rungta, Hyun B. Choi, ..., Terrance P. Snutch, Brian A. MacVicar

Correspondence

bmacvicar@brain.ubc.ca

In Brief

Neuronal swelling, the major cause of death in traumatic and ischemic brain injuries, is initiated when aberrant entry of sodium ions and depolarization activates the voltage-gated chloride channel, SLC26A11. The increase of cytoplasmic sodium and chloride causes an osmotic imbalance that leads to water entry and cytotoxic edema, a mechanism that could be targeted to prevent and treat brain edema.

Rungta et al., 2015, Cell *161*, 610–621
April 23, 2015
http://dx.doi.org/10.1016/j.cell.2015.03.029

CellPress

Cell

Article

The Cellular Mechanisms of Neuronal Swelling Underlying Cytotoxic Edema

Ravi L. Rungta,[1] Hyun B. Choi,[1] John R. Tyson,[1,2] Aqsa Malik,[1] Lasse Dissing-Olesen,[1] Paulo J.C. Lin,[3] Stuart M. Cain,[1,2] Pieter R. Cullis,[3] Terrance P. Snutch,[1,2] and Brian A. MacVicar[1,*]

[1]Djavad Mowafaghian Centre for Brain Health, University of British Columbia, Vancouver, BC V6T 2B5, Canada
[2]Michael Smith Laboratories, University of British Columbia, Vancouver, BC V6T 1Z4, Canada
[3]Department of Biochemistry and Molecular Biology, University of British Columbia, Vancouver, BC V6T 1Z3, Canada
*Correspondence: bmacvicar@brain.ubc.ca
http://dx.doi.org/10.1016/j.cell.2015.03.029

SUMMARY

Cytotoxic brain edema triggered by neuronal swelling is the chief cause of mortality following brain trauma and cerebral infarct. Using fluorescence lifetime imaging to analyze contributions of intracellular ionic changes in brain slices, we find that intense Na^+ entry triggers a secondary increase in intracellular Cl^- that is required for neuronal swelling and death. Pharmacological and siRNA-mediated knockdown screening identified the ion exchanger SLC26A11 unexpectedly acting as a voltage-gated Cl^- channel that is activated upon neuronal depolarization to membrane potentials lower than −20 mV. Blockade of SLC26A11 activity attenuates both neuronal swelling and cell death. Therefore cytotoxic neuronal edema occurs when sufficient Na^+ influx and depolarization is followed by Cl^- entry via SLC26A11. The resultant NaCl accumulation causes subsequent neuronal swelling leading to neuronal death. These findings shed light on unique elements of volume control in excitable cells and lay the ground for the development of specific treatments for brain edema.

INTRODUCTION

Brain edema, the pathological hallmark of excitotoxic injury and traumatic brain injury (Donkin and Vink, 2010; Klatzo, 1987; Marmarou et al., 2006; Rosenblum, 2007) was first characterized by Klatzo (1967) as either vasogenic or cytotoxic. Cytotoxic brain edema is caused by water movement into the intracellular compartment of neurons and/or astrocytes leading to brain swelling, while vasogenic edema is due to water entry into the brain from the vasculature (Klatzo, 1967). Excitotoxic swelling of cultured neurons is known to involve influx of both Na^+ and Cl^-, although the influx pathway(s) for Cl^- remain obscure (Choi, 1987; Hasbani et al., 1998; Rothman, 1985). The low resting Cl^- permeability in neurons suggests that a Cl^- channel or exchange mechanism must be activated for Cl^- entry to occur at sufficient levels to increase cell volume and cause cytotoxic edema. In mature pyramidal neurons of the cortex and hippocampus, the equilibrium potential for Cl^- (E_{Cl^-}) is set more hyperpolarized to the resting membrane potential (E_m) by KCC2-mediated active transport of Cl^- out of the cell against its electrochemical concentration gradient (Blaesse et al., 2009). As such, the Cl^- influx required for cytotoxic neuronal edema occurs as a result of either the activation of a Cl^- channel that is not open at rest, or activation of a Cl^- transporter. Putative candidates for Cl^- loading leading to swelling are the volume-regulated anion channel (VRAC), the Na^+-K^+-Cl^- co-transporter 1 (NKCC1) and GABA-activated Cl^- channels (Allen et al., 2004; Hasbani et al., 1998; Inoue et al., 2005; Pond et al., 2006). In addition, there are several newly described Cl^- channels and transporters that could also be important contributors to neuronal edema. Our experiments were designed to examine the interrelationship between neuronal volume, intracellular Na^+ concentration ($[Na^+]_i$) and intracellular Cl^- concentration ($[Cl^-]_i$) in order to investigate the roles for Cl^- entry pathways that contribute to neuronal swelling leading to cell death.

Neuronal swelling occurs as a result of multiple depolarizing triggers that increase $[Na^+]_i$ including excessive glutamate receptor activation, intense neuronal spiking, activation of non-selective cation channels, and inhibition of Na^+/K^+-ATPase (Liang et al., 2007). We tested the impact of increasing $[Na^+]_i$ via ligand- or voltage-gated ion channels on neuronal swelling to test the hypothesis that extensive Na^+ influx itself, independent of the route of entry, leads to swelling by triggering Cl^- influx. Two-photon imaging of cell morphology and fluorescence lifetime measurements (FLIM) of $[Na^+]_i$ and $[Cl^-]_i$ in hippocampal and cortical neurons in acutely prepared brain slices were combined to specifically examine the relationship between increased $[Na^+]_i$, subsequent $[Cl^-]_i$ changes, and neuronal swelling. The cytotoxic nature of this swelling was measured by lactate dehydrogenase (LDH) efflux (e.g., Kajta et al., 2005). Pharmacological blockers of known Cl^- channels and exchangers were further examined in order to determine the relative contribution of different Cl^- loading pathways to neuronal swelling. Finally, a lipid nanoparticle (LNP) strategy to introduce siRNA into neurons in vivo (Rungta et al., 2013) was employed to determine the exact Cl^- pathway critical and required for the majority of neuronal swelling. The results indicate that a significant proportion of neuronal swelling and subsequent cell death requires SLC26A11, a protein that can act as a Cl^-, HCO_3^-, SO_4^- exchanger or a Cl^- channel in expression systems and recently

reported to be highly expressed in cortical and hippocampal neurons (Rahmati et al., 2013). The identification of the principal pathway required for Cl^- entry could potentially lead to novel targets and therapies for treating cytotoxic brain edema.

RESULTS

Increased Intracellular Sodium Triggers Neuronal Swelling

We first investigated whether increasing $[Na^+]_i$ was itself capable of triggering a cascade leading to an increase in cell volume and second whether this cascade also leads to rapid cell death. Two parallel and independent approaches were taken to increase $[Na^+]_i$ by either applying veratridine, which removes inactivation of voltage-gated sodium channels (VGSCs) (Strichartz et al., 1987) prolonging Na^+ entry or by applying NMDA to activate NMDA receptors (NMDARs). NMDA activates a non-selective cation conductance leading to entry of Na^+ and also Ca^{2+}. Neuronal Na^+ entry was induced under conditions in which other voltage-gated ion channels and ligand-gated transmitter receptors were blocked by a combination of Cd^{2+} (30 μM), CNQX (20 μM) and picrotoxin (100 μM). Either veratridine or NMDA was rapidly applied by pressure ejection from a pipette positioned directly above the region of the brain slice that was imaged. To ensure the selectivity of either approach veratridine was applied with d-APV (100 μM) to block NMDARs and NMDA was applied with TTX (1 μM) to block VGSCs. Changes in $[Na^+]_i$ were monitored using the fluorescent Na^+ indicator CoroNa-Green (Meier et al., 2006), which preferentially stains hippocampal and cortical neurons in brain slices (Figure 1A). Astrocytes, which did not show any obvious volume changes under these experimental manipulations, were visualized using Sulforhodamine 101 (SR101) (Nimmerjahn et al., 2004) to provide landmarks to track during swelling of the tissue (red cells in Figures 1A and 1B). The activation of either VGSCs by veratridine or NMDARs by NMDA consistently led to a significant increase in $[Na^+]_i$ followed, after a delay of seconds, by an increase in neuronal cell volume (Figures 1B–1D, 1J, 1K, 2A, and 2B and Movie S1). We further compared the impact of Ca^{2+} versus Na^+ entry through NMDARs on swelling by repeating experiments in Ca^{2+} or Na^+ free extracellular solutions. The increase in cell volume from NMDAR activation was still observed in extracellular Ca^{2+} free solution (cross sectional area increased to 161.60% ± 10.55% of baseline). However, in the presence of low concentration of extracellular Na^+ ($[Na^+]_{ext}$) and normal Ca^{2+}, swelling was completely absent and NMDAR activation actually resulted in a decrease in neuronal volume (Figures 1J, 2C, and 2D). Control experiments showed that neuronal $[Na^+]_i$ increases and swelling induced by veratridine were blocked by the VGSC antagonist, TTX (Figures 1J and 1K; $p < 0.001$, two-tailed Student's t test) and those induced by NMDA were blocked by the NMDAR antagonist, d-APV (Figures 1J and 1K; $p < 0.001$, ANOVA). Our experimental assay was performed at room temperature to facilitate the imaging of AM indicator dyes which are more rapidly extruded from neurons at 37°C (Beierlein et al., 2004) (Figure S1). However, as the function of many transporters and metabolic proteins that govern ion transport are temperature-dependent, we confirmed that increases in $[Na^+]_i$ equally cause swelling of neurons at 37°C (Figure S1).

Although an increase in Na^+ preceding swelling was consistently observed, the magnitude and duration of CoroNa fluorescence signals were distorted during cellular swelling due to dye dilution. This is consistent with our observations that swelling was associated with reduced fluorescence intensity of the inert dye, Calcein red-AM (Figure S2). However, without the ability to dissociate changes in $[Na^+]_i$ from changes in dye concentration, it is not possible to conclude that $[Na^+]_i$ itself is not also decreasing during swelling. In order to define the true magnitude and time course of the $[Na^+]_i$ increases, we developed a method to record real-time calibrated measurements of $[Na^+]_i$ using two-photon FLIM which was independent of changes in dye concentrations. When lifetime measurements of CoroNa were first tested in iso-osmotic salt solutions the time constant of decay (τ) increased with increasing $[Na^+]$ (Figure 1G). However, as the local environment can affect lifetime measurements of dyes (Berezin and Achilefu, 2010), calibrations of CoroNa lifetimes were obtained within the cytoplasm of neurons by whole-cell voltage-clamping of neurons and dialysis with different $[Na^+]$ concentrations. CoroNa lifetimes were best fit using a biexponential decay (Figure S3) with a short lifetime (τ_{fast}) predictive of $[Na^+]_i$ (Figures 1H and 1I). FLIM of CoroNa loaded neurons revealed that $[Na^+]_i$ increased to approximately 94.46 ± 2.14 mM (calibrated value) throughout veratridine application and gradually recovered after washout (Figures 1E and 1F and Movie S2). These results demonstrate that the decrease in CoroNa fluorescence as the neurons swell is primarily due to dye dilution and not a dilution of $[Na^+]_i$ itself.

Cl^- Influx Is Required for Na^+-Induced Neuronal Swelling

Since cytoplasmic impermeant anions make up the bulk of the intracellular anionic milieu, changes in $[Cl^-]_i$ must be met by an accompanying influx of water, possibly via transporters (Zeuthen, 2010), in an attempt to achieve Gibbs-Donnan equilibrium (Glykys et al., 2014). We therefore examined whether prolonged $[Na^+]_i$ increases were associated with a secondary influx of Cl^-, and further whether Cl^- entry was ultimately required for neuronal swelling. Using two-photon FLIM of the Cl^--sensitive dye MQAE (Ferrini et al., 2013; Verkman et al., 1989), we observed that $[Cl^-]_i$ increased in neurons (indicated by a decrease in the fluorescence lifetime) when Na^+ influx was triggered by veratridine application (Figures 3A and 3B). This Cl^- influx was independent of entry via $GABA_A$Rs as all experiments were performed in the presence of the ligand-gated Cl^- channel antagonist, picrotoxin (100 μM).

Whether neuronal Na^+ and subsequent Cl^- influx was sufficient to increase tissue volume were next investigated by imaging hippocampal/cortical brain slices at low magnification. Application of veratridine triggered dramatic swelling of brain slices that was reduced but still substantial even when a number of Na^+, Ca^{2+}, and Cl^- entry pathways were reduced by blockade of glutamate-gated AMPARs and NMDARs, voltage-gated Ca^{2+} channels (VGCCs), and GABA activated Cl^- channels with a cocktail of blockers (20 μM CNQX, 100 μM d-APV, 30 μM Cd^{2+}, and 100 μM picrotoxin) (Figures 3C and 3D and Movie

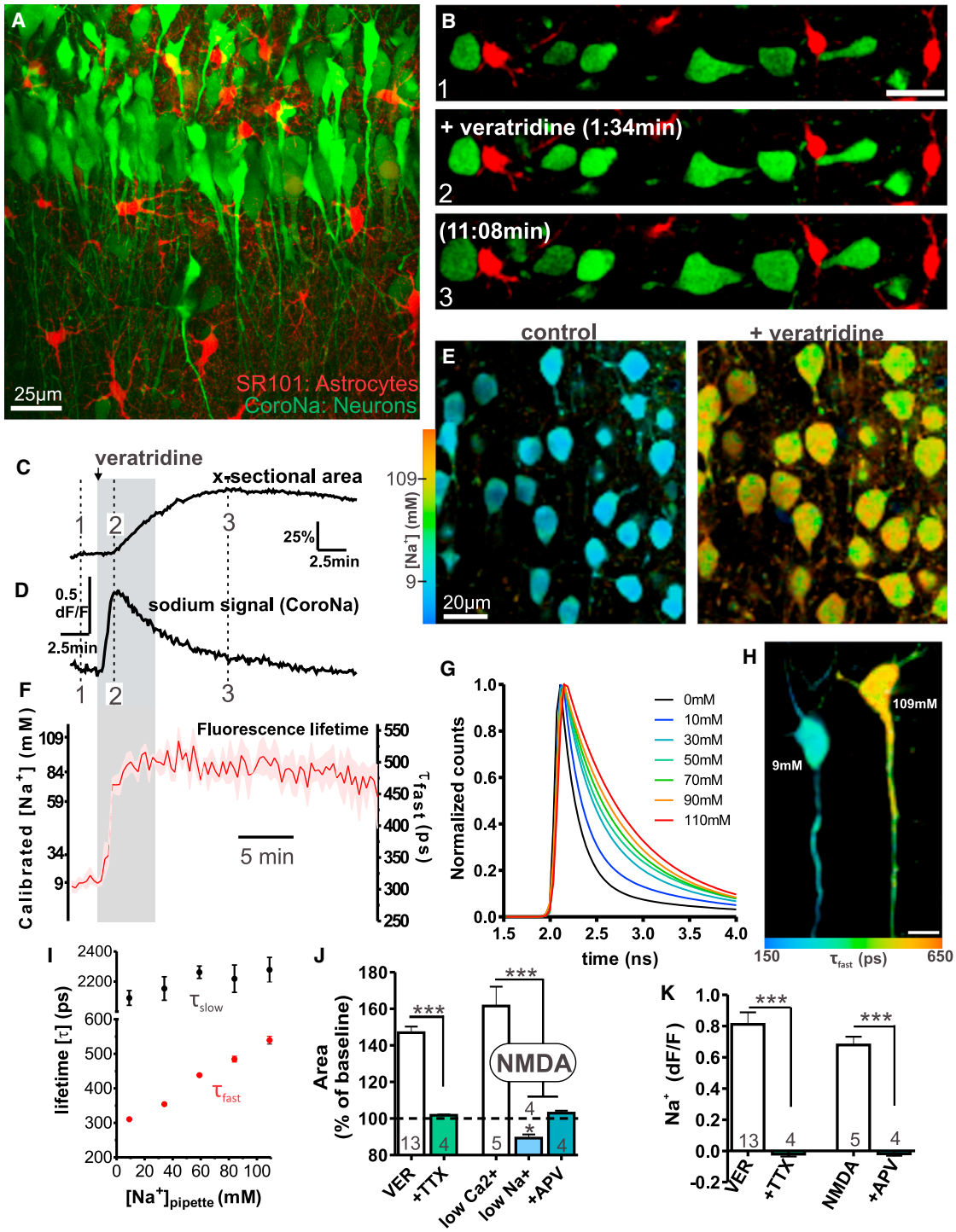

Figure 1. Neuronal Swelling Is Caused by Prolonged Increases in Intracellular Na^+ and Is Independent of Ca^{2+}

(A) CoroNa Green (Na^+ indicator) loaded neurons versus SR101 stained astrocytes (red) in a hippocampal brain slice imaged using two-photon laser scanning microscopy.

(B–D) Cortical neurons treated with veratridine (50 µM) show increase in $[Na^+]_i$ followed by swelling (increase in cross sectional area). Astrocytes do not swell.

(E and F) CoroNa FLIM measurements of $[Na^+]_i$ as neurons swell reveals true time course and magnitude of Na^+ signals that are independent of dye concentration (n = 4).

(G–I) Calibration of FLIM measurements of neuronal $[Na^+]_i$ with CoroNa. (G) Decay of CoroNa fluorescence changes in salt solutions with varying $[Na^+]$. (H) Dual (simultaneous) whole-cell patch clamping of two neurons dialyzed with high (109 mM) and low (9 mM) $[Na^+]_i$ show distinct separation of lifetimes. (I) Calibration of

(legend continued on next page)

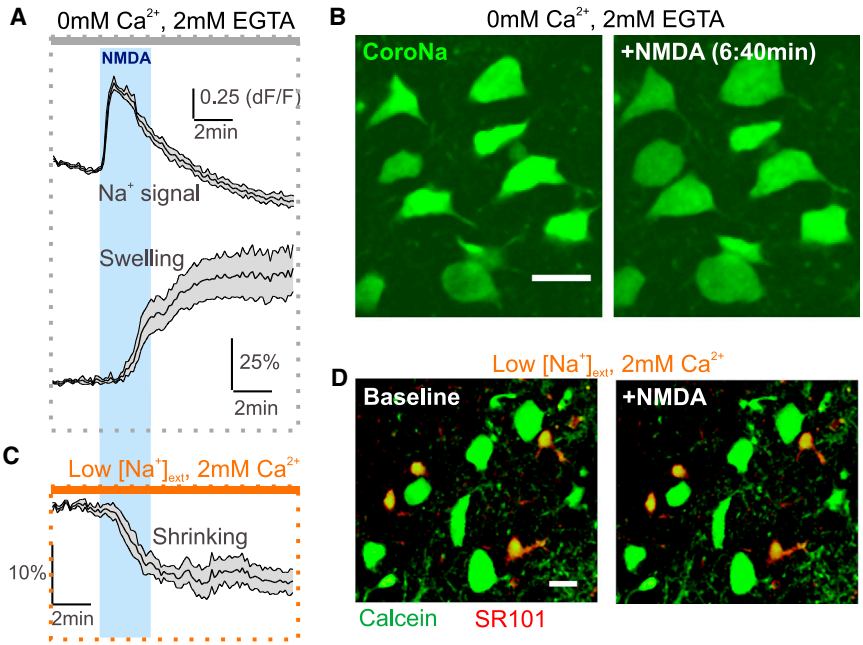

Figure 2. NMDAR Activation Triggers Neuronal Swelling that Requires Na^+ Influx, but That Is Independent of Ca^{2+} Influx

(A and B) Na^+ influx triggers an increase in neuronal volume, measured as the cross sectional area in the absence of extracellular Ca^{2+} (0 mM Ca^{2+}, 2 mM EGTA) (n = 5).

(C and D) Iso-osmotic replacement of extracellular Na^+ with NMDG (from 152 mM to 26 mM), to reduce Na^+ entry through NMDARs prevents neurons from swelling and causes them to shrink (86.7% of baseline, $p < 0.05$) (n = 4).

Scale bars, 15 μm (B and D). Shaded area above and below mean represent SEM.

S3). In contrast, blocking all Cl^- influx pathways by reducing the concentration of extracellular Cl^- ($[Cl^-]_{ext}$) with iso-osmotic replacement of NaCl for Na-gluconate in the extracellular solution dramatically reduced the magnitude of the volume increase of brain slices (Figure 3D; $p < 0.001$, ANOVA). These results suggest that even when fast ionotropic glutamate and GABA activated receptors are blocked, increased neuronal $[Na^+]_i$ leads to cytotoxic edema of brain tissue that is dependent on Cl^- influx. We next tested whether reducing $[Cl^-]_{ext}$ also prevented Na^+-induced swelling of individual neurons. Indeed, reducing $[Cl^-]_{ext}$ reduced the swelling of neurons visualized with CoroNa fluorescence (Figures 3E and 3F and Movie S4; $p < 0.001$, ANOVA), without affecting the $[Na^+]_i$ signal (Figure 3H; $p > 0.05$, two-tailed Student's t test). As it has been previously reported that $GABA_AR$-mediated Cl^- influx can contribute to both neuronal swelling in cell culture (Hasbani et al., 1998) and to swelling following oxygen glucose deprivation in situ (Allen et al., 2004), the contribution of $GABA_AR$ Cl^- influx to neuronal swelling in our experimental conditions was examined. Consistent with previous reports, pre-application of the $GABA_AR$ antagonist picrotoxin slightly but significantly reduced the magnitude of neuronal swelling (from 161.7% to 146.9%; Figure 3F; $p < 0.05$, ANOVA); however, the majority of the volume increase persisted in picrotoxin suggesting that the cause of swelling was dominated by Cl^- influx via an as yet unidentified mechanism. NMDA-induced swelling was also blocked by low $[Cl^-]_{ext}$ (iso-osmotic replacement of NaCl for Na-isethionate) (Figure 3G; $p < 0.05$, two-tailed Student's t test). Together, these data indicate that neuronal swelling requires Cl^- influx through a mechanism that is triggered by an increase in $[Na^+]_i$ and that Na^+ entry alone is not sufficient to swell neurons.

Na^+ and Cl^- Dependent Neuronal Swelling Causes Death

Aberrant calcium influx via NMDARs can lead to mitochondrial depolarization and cell death; however, Cl^- removal also reduces ischemia- and glutamate-evoked early neuronal death in cell culture (Choi, 1987; Goldberg and Choi, 1993; Rothman, 1985), suggesting the existence of two independent pathways ultimately leading to cell death. The impact of the $[Na^+]_i$-triggered Cl^- entry and neuronal swelling on cell viability was further investigated using LDH release as a measure of cell death (e.g. Kajta et al., 2005). Even in the combined presence of CNQX, picrotoxin, and Cd^{2+} to block fast AMPA/KA receptors, GABA-activated Cl^- channels, and VGCCs, respectively, application (15 min) of either veratridine (50 μM) or NMDA (100 μM, in artificial cerebrospinal fluid [ACSF] containing 0 mM Ca^{2+} and 2 mM EGTA) caused a rapid and significant increase in LDH release, indicating neurons were dying after 90 min (Figures 3I and 3J; $p < 0.01$, ANOVA). Both the NMDA-induced and veratridine-induced neuronal death, as indicated by LDH release, were abolished by reducing $[Cl^-]_{ext}$ throughout the experiment (Figures 3I and 3J; $p < 0.01$, ANOVA). This suggests that Na^+-induced Cl^-

CoroNa lifetimes measured in soma of neurons dialyzed with different $[Na^+]$ shows that the $[Na^+]_i$ can be predicted from τ_{fast}. Calibrated values for each $[Na^+]$ were obtained from $n \geq 3$ voltage clamped neurons.

(J and K) Quantified data show neuronal swelling is triggered by sodium influx via independent pathways. NMDAR-mediated swelling was dependent on Na^+ influx and independent of Ca^{2+}. Control confirms Na^+ signal and swelling caused by veratridine and NMDA was via VGSCs and NMDARs respectively, as they were blocked by antagonists, TTX (1 μM) and d-APV (100 μM).

All experiments were done in the presence of 30 μM Cd^{2+}, 20 μM CNQX, 100 μM picrotoxin. Additionally, neurons were pretreated with 100 μM d-APV (NMDAR antagonist) for veratridine experiments and 1 μM TTX (VGSC antagonist) for NMDA experiments to confirm pathways were independent. Scale bars, 20 μm (B) and 15 μm (H). VER, veratridine; x-sectional, cross sectional; VGSC, voltage-gated sodium channel; SR101, sulforhodamine 101. Control values in (J) and (K) are also re-plotted in Figures 3 and 4. Error bars and shaded region above and below the mean represent SEM. See also Figure S1, S2, and S3 and Movie S1, S2, and S3.

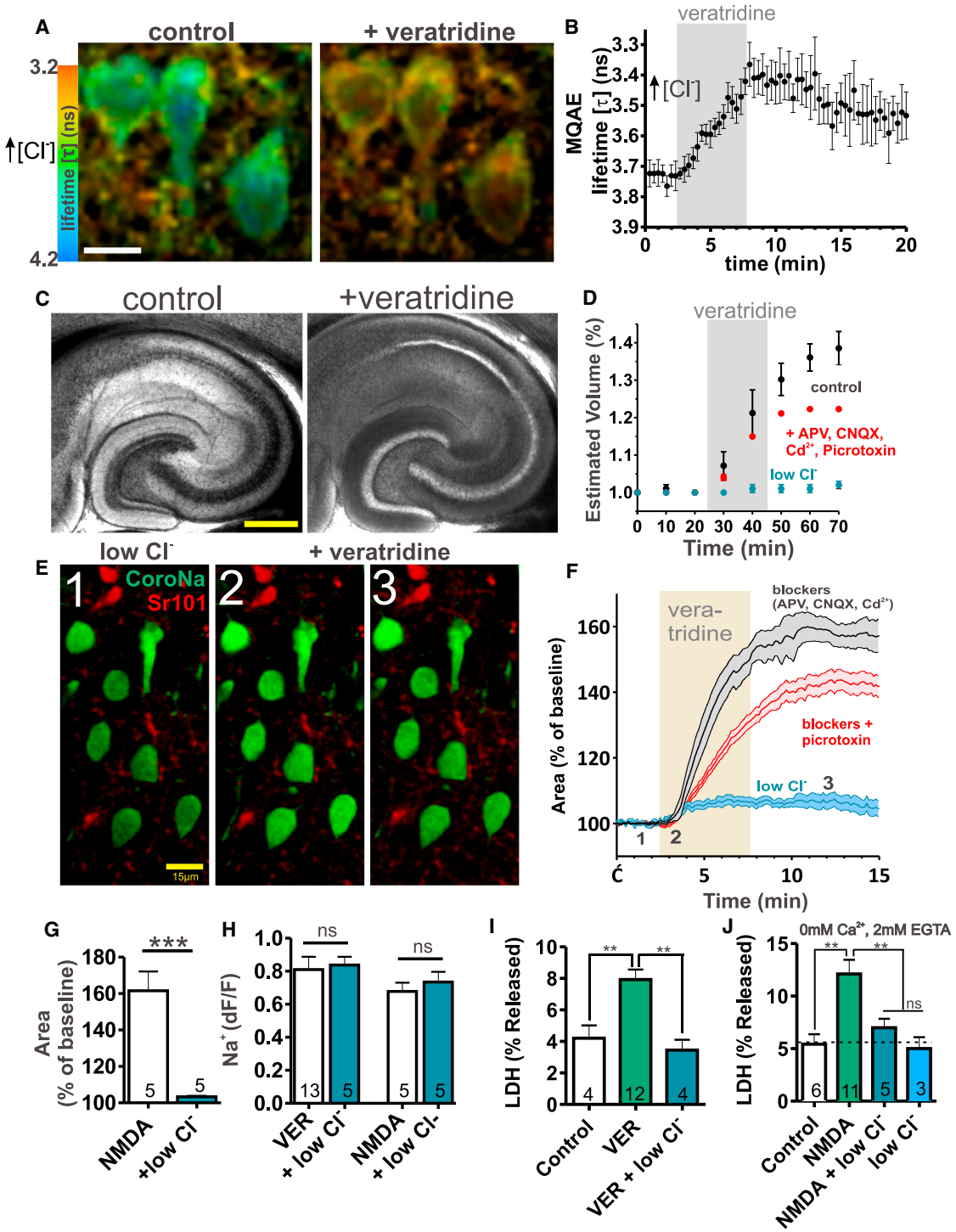

Figure 3. Na^+ Influx Is Correlated with a Secondary Cl^- Influx That Is Required for Neuronal Swelling and Causes Cell Death

(A and B) FLIM of Cl^--sensitive dye, MQAE, shows that Cl^- influx is correlated with increases in $[Na^+]_i$ (n = 5).

(C and D) Neuronal Na^+ influx triggers an increase in brain tissue volume shown by changes in volume of a hippocampal brain slice. (D) Cocktail of fast glutamate receptor, GABA receptor and VGCC blockers slightly reduce tissue swelling ($p < 0.01$) but significant Cl^- dependent swelling still occurs ($p < 0.01$) indicating that swelling is dominated by other mechanisms.

(E and F) Veratridine triggered neuronal swelling is prevented by reducing extracellular Cl^- (10.5 mM) and is only partially inhibited by blocking $GABA_A$Rs.

(G) NMDA triggered swelling is blocked by reducing extracellular Cl^-.

(H) Positive control shows veratridine and NMDAR Na^+ signals were unaffected by low Cl^- solution.

(legend continued on next page)

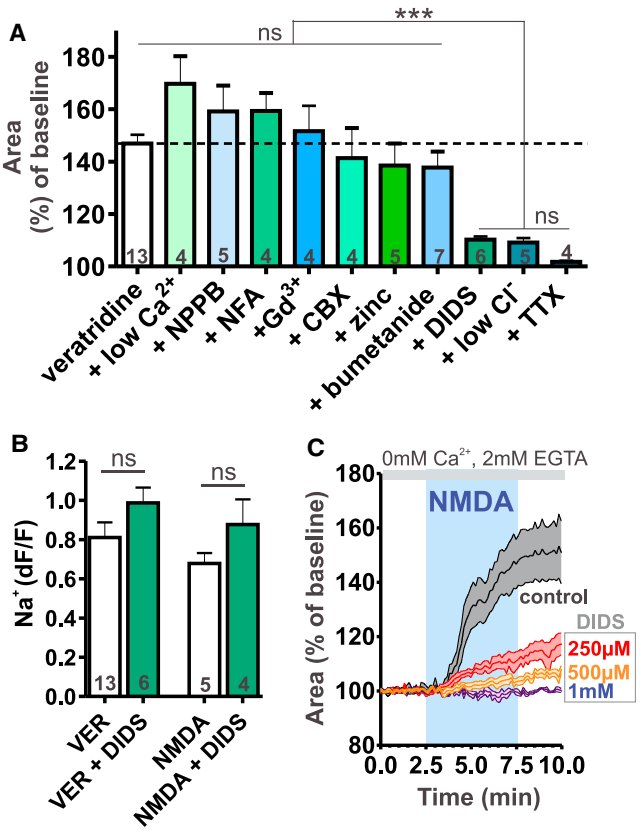

Figure 4. Neuronal Swelling Reflects the Pharmacological Profile of a SLC4 or SLC26 Family Member

(A) Veratridine-induced neuronal swelling was blocked by the HCO_3^- /Cl^- exchanger inhibitor, DIDS (250 μM) but not by blockers of several other Cl^-channels or transporters (see Table S1).

(B) Positive control shows veratridine and NMDA-induced Na^+ signal in the presence of DIDS.

(C) NMDA-induced neuronal swelling was blocked by DIDS in a dose dependent manner; control (n = 5), 250 μM (n = 4), 500 μM (n = 5), 1 mM (n = 5). All solutions contained blockers: 30 μM Cd^{2+}, 20 μM CNQX, 100 μM picrotoxin, plus either 100 μM d-APV for veratridine experiments or 1 μM TTX for NMDA experiments. VER, veratridine. Error bars and shaded region above and below the mean represent SEM.

influx and subsequent swelling results in Ca^{2+}-independent cell death.

Pharmacological Analyses of the Predominant Cl^- Influx Pathway Required for Neuronal Swelling and Death

There are several candidates for the transmembrane influx of Cl^- in neurons that can be distinguished based on their sensitivity to different antagonists (Alvarez-Leefmans and Delpire, 2009; Jentsch et al., 2002; Verkman and Galietta, 2009) (Table S1). We hypothesized that by identifying and blocking the source of Cl^- entry that was triggered by Na^+ entry, both the Na^+-induced neuronal swelling and corresponding cell death could be prevented. As a first step, pharmacological analyses using the imaging assay of swelling of neurons in brain slices were undertaken in order to screen for the possible involvement of different Cl^- channels and transporters. In separate experiments the following blockers were tested as described in Table S1; NPPB (200 μM) to block the volume-regulated anion channel (VRAC, VSOR), zinc (300 μM) to block CLC-2, Gd^{3+} (100 μM) to block the Maxi-anion channel, niflumic acid (NFA) (200 μM) to block the Ca^{2+} activated Cl^- conductance (CaCC, bestrophin), carbenoxelone (CBX) (100 μM) to block pannexins/connexins, bumetanide (100 μM) to block cation chloride cotransporters (NKCC1 and KCC2), and DIDS (250 μM) to block SLC4 and SLC26 anion exchangers. All antagonists were both bath applied and present in the puffing pipette used to apply either NMDA or veratridine. Of note, of the various Cl^- channel and transporter blockers examined, only DIDS reduced the swelling induced by increased $[Na^+]_i$ (Figure 4A; $p < 0.05$ compared to all other antagonists, ANOVA). The small volume change in the presence of DIDS was not significantly different from those observed in low Cl^- extracellular solution (Figure 4A; $p > 0.05$, ANOVA). A substantial $[Na^+]_i$ increase was still observed in DIDS indicating that Na^+ entry was not affected (Figure 4B). This pattern of block by DIDS but no effect of the numerous other blockers suggested that a member of the SLC4 or SLC26 families of anion exchangers was the most likely source of Cl^- entry. Although DIDS also blocks VRAC, which has been implicated in excitotoxic cell death in neuronal cell culture (Inoue and Okada, 2007), under our conditions we observed no protection of either cell volume or cell death in the presence of the potent VRAC blocker, NPPB. DIDS also blocked NMDA-evoked neuronal swelling in a dose-dependent manner (Figure 4C) and was confirmed to block the veratridine-stimulated swelling at 37°C (Figure S1), suggesting a common mechanism.

As it was observed that extracellular Cl^- was required for both neuronal swelling and the subsequent cell death and that DIDS prevented neuronal swelling, we predicted that DIDS would block the Cl^- dependent cell death pathway without affecting the classic Ca^{2+}-dependent death. DIDS was initially tested for its effectiveness in preventing the swelling-induced, Cl^--dependent cell death as measured by LDH efflux in brain slices exposed to veratridine. Indeed, DIDS prevented cell death from veratridine-induced Na^+ influx and swelling (Figure 5A; $p < 0.005$, ANOVA), whereas the VRAC blocker NPPB had no effect. DIDS was further examined on both the NMDA

(I) Neuronal Na^+ influx via VGSCs causes cell death that is Cl^--dependent as measured by LDH release.

(J) Neuronal Na^+ influx via NMDARs causes cell death that is Cl^--dependent and Ca^{2+}-independent. Slices were incubated in low $[Cl^-]_o$ or control ACSF for the entire experiment starting 20 min. prior to either Veratridine or NMDA (15 min.). LDH was collected from supernatant 1.5 hr following end of Veratridine or NMDA treatment.

Scale bars, 10 μm (A), 1.0 mm (C), 15 μm (E). For experiments in (A, B, E and G–J) solutions contained blockers: 30 μM Cd^{2+}, 20 μM CNQX, 100 μM picrotoxin, plus either 100 μM d-APV for veratridine experiments or 1 μM TTX for NMDA experiments. n values in (F), blockers (n = 5), +picrotoxin (n = 13), low Cl^- (n = 5). VER, veratridine; VGCC, voltage-gated calcium channel; VGSC, voltage-gated sodium channel. Error bars and shaded region above and below the mean represent SEM. See also Movie S3 and Movie S4.

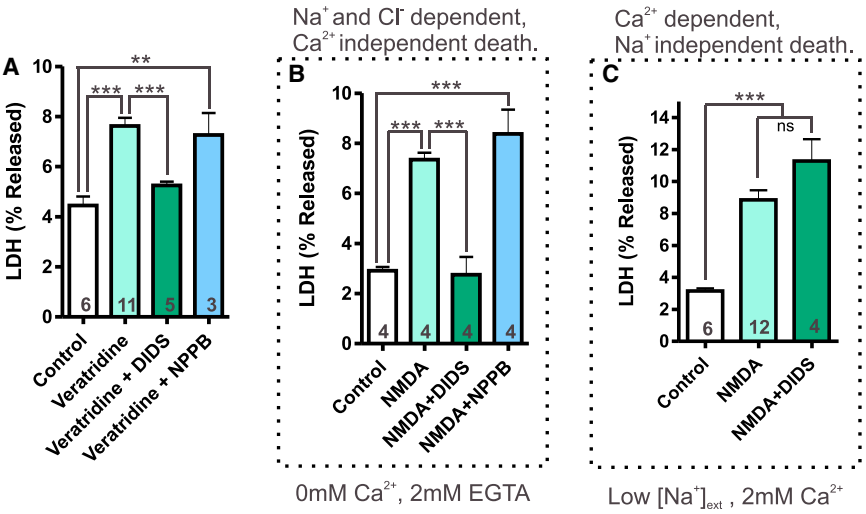

Figure 5. DIDS Blocks Na^+ and Cl^- Dependent, Ca^{2+} Independent Cell Death

(A) LDH release measurements show Na^+- and Cl^--dependent cell death triggered by veratridine was blocked by the HCO_3^-/Cl^- exchanger antagonist, DIDS but not by the VRAC blocker NPPB.

(B) NMDAR Na^+ influx triggers cell death in the absence of extracellular Ca^{2+} that is blocked by DIDS but not NPPB.

(C) NMDAR Ca^{2+} influx also triggers cell death that is not blocked by DIDS, indicating separate pathways. Error bars above and below the mean represent SEM.

Cl^--dependent, Ca^{2+}-independent cell death pathway and on the NMDA Ca^{2+}-dependent cell death pathway. As predicted, DIDS blocked the cell death caused by NMDA in Ca^{2+} free extracellular solution (Figure 5B; $p < 0.005$, ANOVA). If however, NMDA was applied in the presence of extracellular Ca^{2+} but reduced extracellular Na^+, cell death still occurred (Figure 5C; $p < 0.005$, ANOVA) but was not blocked by DIDS (Figure 5C; $p > 0.05$, ANOVA). These results suggest that two independent cell death pathways co-exist that can be distinguished based on their ionic basis; one that involves swelling, requires Na^+ and Cl^- influx, is Ca^{2+} independent, and is blocked by DIDS, and one that is triggered by Ca^{2+} influx, but that is not DIDS sensitive.

Identification of SLC26A11 as the Predominant Cl^- Influx Pathway Underlying Na^+ Dependent Cytotoxic Neuronal Swelling

Our data indicate that Na^+ entry into neurons is linked to a DIDS-sensitive Cl^- influx pathway that is required for neuronal swelling and mediates cell death. Several DIDS-sensitive candidates are expressed in CNS neurons of which several act as Cl^-/HCO_3^- exchangers and include the SLC4 family of exchangers (Alvarez-Leefmans and Delpire, 2009; Boron et al., 2009; Romero et al., 2013). The DIDS-sensitive Cl^-, HCO_3^- exchangers that are known to be expressed in the cortex and hippocampus are SLC4A3, SLC4A8, and SLC4A10 (Boron et al., 2009; Romero et al., 2013). In addition, SLC26A11 was recently shown to be highly expressed in CNS cortical neurons (Rahmati et al., 2013). SLC26A11 is a member of the sulfate transporter family that in different expression systems has been reported to act variously as a DIDS-sensitive sulfate transporter, a DIDS-sensitive exchanger for Cl^-, SO_4^{2-}, HCO_3^-, or H^+-Cl^- or as a Cl^- channel (Lee et al., 2012; Rahmati et al., 2013; Vincourt et al., 2003; Xu et al., 2011).

Utilizing qRT-PCR, the expression of SLC4 and SLC26 family members was confirmed in both cortical and hippocampal brain tissue (Figure S4). Based on their combined pharmacological profile and expression profiles, SLC4-A3, -A8, -A10, and SLC26A11 appeared to be the most promising candidates for the Cl^- entry pathway that causes neuronal swelling. We recently reported the development of an efficient LNP-mediated delivery system to introduce siRNAs against specific molecular targets into CNS neurons both in vivo and in vitro (Rungta et al., 2013). Individual siRNAs targeted against the different SLC candidate genes were encapsulated in DiI labeled LNPs and initially tested for their ability to attenuate expression in both primary neuron cultures and a HEK cell expression system (Figure S4. These in vitro-validated siRNA LNPs against the 4 different SLC candidates or a control (luciferase) siRNA were subsequently injected intracranially into the rat somatosensory cortex. After allowing 5-6 days for uptake of LNPs and knockdown of candidate proteins to occur, neurons that had taken up DiI labeled LNPs were examined for Na^+-induced Cl^--dependent swelling in cortical slices. Knockdown of SLC4A-3, −8, or −10 either separately or together had no significant effect on the magnitude of veratridine-induced neuronal swelling compared to the control luciferase siRNA injected animals (Figures 6C and 6G and S5; $p > 0.05$, ANOVA). In striking contrast, knockdown of SLC26A11 with two siRNAs targeted toward different sequences of SLC26A11 mRNA, significantly reduced the magnitude of the swelling in neurons (Figures 6D and 6H and Movie S5; $p < 0.05$, ANOVA was performed comparing results from all siRNA groups (luciferase, A3, A8, A10, A3+A8+A10, A11 No.1 and A11 No.2)). The occurrence of SLC26A11 knockdown was further validated by western blot analysis of SLC26A11 protein in tissue 5 days following injection of SLC26A11 siRNA-LNPs (Figures 6A and 6B). These results indicate that the Cl^- influx that is required for neuronal swelling is mediated by a SLC26A11-dependent process.

Studies of the properties of recombinant SLC26A11 have shown that, depending upon the cell type in which it is expressed, this protein can act either as a Cl^- channel or a SO_4^{2-} or oxalate transporter that is inhibited by DIDS or the CFTR antagonist GlyH-101 (Alper and Sharma, 2013; Rahmati et al., 2013; Stewart et al., 2011). We therefore investigated whether GlyH-101 has similar actions on preventing neuronal swelling and the associated cell death and whether there exists a neuronal Cl^- current that is sensitive to both DIDS and GlyH-101. Similar to the actions of DIDS, GlyH-101 profoundly

inhibited both veratridine-stimulated swelling (Figure 6E; $p < 0.001$, two-tailed Student's t test) and cell death (Figure 6F; $p < 0.001$, ANOVA).

The opening of Na^+ permeable channels causes both $[Na^+]_i$ accumulation and neuronal depolarization. The large (~80 mM) increases in $[Na^+]_i$ occurred prior to the increases in cell volume (Figure 1) suggesting that there are compensatory mechanisms such as K^+ efflux that are initially sufficient to maintain osmotic equilibrium. Decreased intracellular K^+ and progressive accumulation of extracellular K^+ could also contribute to further depolarization of the membrane. We therefore tested the possibility that SLC26A11 in cortical neurons is required for a DIDS- and GlyH-101-sensitive Cl^- channel that is opened by depolarization. Such outwardly rectifying, non-inactivating DIDS-sensitive conductances have previously been described in neurons (Smith et al., 1995), although their molecular identity remains unknown. Whole-cell voltage clamp recordings were obtained under conditions to reveal voltage-dependent Cl^- currents by blocking other known voltage-gated channels with a cocktail of blockers. We targeted layer 4 neurons in cortical slices (Figure 7A), the same cell types that were also imaged in the swelling studies described above. Depolarization to −20 mV or greater elicited a non-inactivating Cl^- current that was blocked by DIDS and was not present when external $[Cl^-]$ was reduced (Figures 7C–7E; $p < 0.001$, ANOVA). In addition, dialysis of neurons with GlyH-101 at concentrations that prevented neuronal swelling were found to also inhibit the voltage-dependent Cl^- current and occluded the effect of DIDS (Figures 7D and 7E; $p < 0.001$, ANOVA). Finally, recordings were made from neurons transfected with siRNA against either SLC26A11 or luciferase (control) using LNPs visualized with DiI. We found that knockdown of SLC26A11 attenuated the DIDS and GlyH-101-sensitive Cl^- current (Figures 7C–7E; $p < 0.001$, ANOVA), demonstrating that SLC26A11 protein is a requirement for an outwardly rectifying Cl^- current activated in substantially depolarized neurons.

DISCUSSION

Our results demonstrate that prolonged Na^+ entry via either of two independent pathways (either VGSCs or NMDARs) converge to activate a Cl^- influx pathway via SLC26A11 that is ultimately required for neuronal swelling and subsequent cell death. Unlike $[Na^+]$ whose osmotic influence on the cell can initially be met by a compensating efflux in $[K^+]$, the anionic intracellular milieu of the cell is largely made up of large impermeable anions. As such, increases in $[Cl^-]_i$ likely maintain electroneutrality by retaining Na^+ and K^+ ions intracellularly, thereby increasing intracellular osmolarity and drawing water into the cell.

In mature pyramidal neurons of the cortex and hippocampus, resting membrane potential (E_m) is set positive compared to the equilibrium potential for Cl^- (E_{Cl}^-) suggesting that Cl^- is not passively distributed across the plasma membrane (Alvarez-Leefmans and Delpire, 2009). Changing membrane potential also has little effect on $[Cl^-]_i$ indicating that there is little Cl^- membrane permeability at rest (Thompson et al., 1988). As such, in order for $[Cl^-]_i$ to rapidly increase in neurons either a Cl^- transporter has to be activated or a transmembrane Cl^- channel has to be opened. Membrane depolarization could also further contribute to Cl^- influx by increasing the driving force for Cl^- entry.

Using an siRNA knockdown approach, we identified the molecular nature of the predominant Cl^- influx pathway that is activated following increases in $[Na^+]_i$ and causes neuronal cytotoxic edema. Our study demonstrates that SLC26A11 acts as a functional Cl^- influx pathway in neurons. A recent study showed that SLC26A11 protein is expressed in neurons throughout the brain and we would predict that similar mechanisms of swelling and neuronal death likely occur in many other areas such as the cerebellum where expression levels are high (Rahmati et al., 2013). SLC26A11, originally identified as a sulfate transporter has been shown to operate in several modes, including an exchanger for Cl^- SO_4^{2-}, HCO_3^-, or H^+-Cl^- or as a Cl^- channel, depending upon the tissue type and the expression system (Rahmati et al., 2013; Vincourt et al., 2003; Xu et al., 2011). The mechanism linking Na^+ influx and SLC26A11-mediated Cl^- influx is most simply explained by membrane depolarization activating SLC26A11 in its Cl^- channel mode, thereby leading to a sustained Cl^- influx. Our observation that SLC26A11 is required for Cl^- channel activity (Rahmati et al., 2013) that opens with depolarizations greater than −20 mV suggests that Cl^- would be constantly entering the cell as E_{Cl}^- in mature neurons is initially set close to −70 mV. During sustained depolarization E_{Cl}^- would drift to more depolarized potentials therefore Cl^- influx would continue until equilibrium is met or the membrane repolarizes. Interestingly, depolarization of cortical neurons with high K^+ solution (40 mM) is not sufficient to cause neuronal swelling alone, and only causes swelling when spreading depression occurs, concurrent with depolarizations to approximately 0 mV and substantial extracellular K^+ accumulation (Zhou et al., 2010; Zhou et al., 2013). A similar breakdown of ionic gradients occurs during pathological settings of cytotoxic edema, such as ischemia, when activation of voltage-gated and ligand-gated channels leads to massive increases in $[Na^+]_i$, followed by increases in extracellular K^+ and almost complete depolarization of the neurons (Dreier, 2011; Somjen, 2001).

Several questions arise as to the specific conditions and times that SLC26A11 may modulate local and global Cl^- concentrations. Aberrant, Cl^- homeostasis is central to several neurological diseases, and it would therefore be interesting to examine whether SLC26A11 expression or localization changes under such conditions. Epileptic seizures are commonly observed in patients following severe traumatic brain injury (TBI) (Annegers et al., 1998; Hung and Chen, 2012; Salazar et al., 1985). Increased $[Cl^-]_i$ leading to a depolarizing shift in E_{GABA} (Cohen et al., 2002; Miles et al., 2012) has been reported to contribute to the generation of seizure activity. If blocking SLC26A11 reduces the increases in Cl^- that occur during pathologies that are associated with cytotoxic edema, it may be possible to maintain the direction of hyperpolarizing $GABA_AR$ currents and reduce the generation of post-traumatic seizures.

In addition to the Cl^- loading that occurs during excitotoxic insults, Cl^- efflux may also be compromised. As KCC2 directional transport is dependent on the K^+ gradient, small changes in extracellular K^+ can have substantial effects on KCC2-mediated Cl^- clearance. Additionally, a recent study demonstrated that glutamate activation of NMDARs leads to phosphorylation and

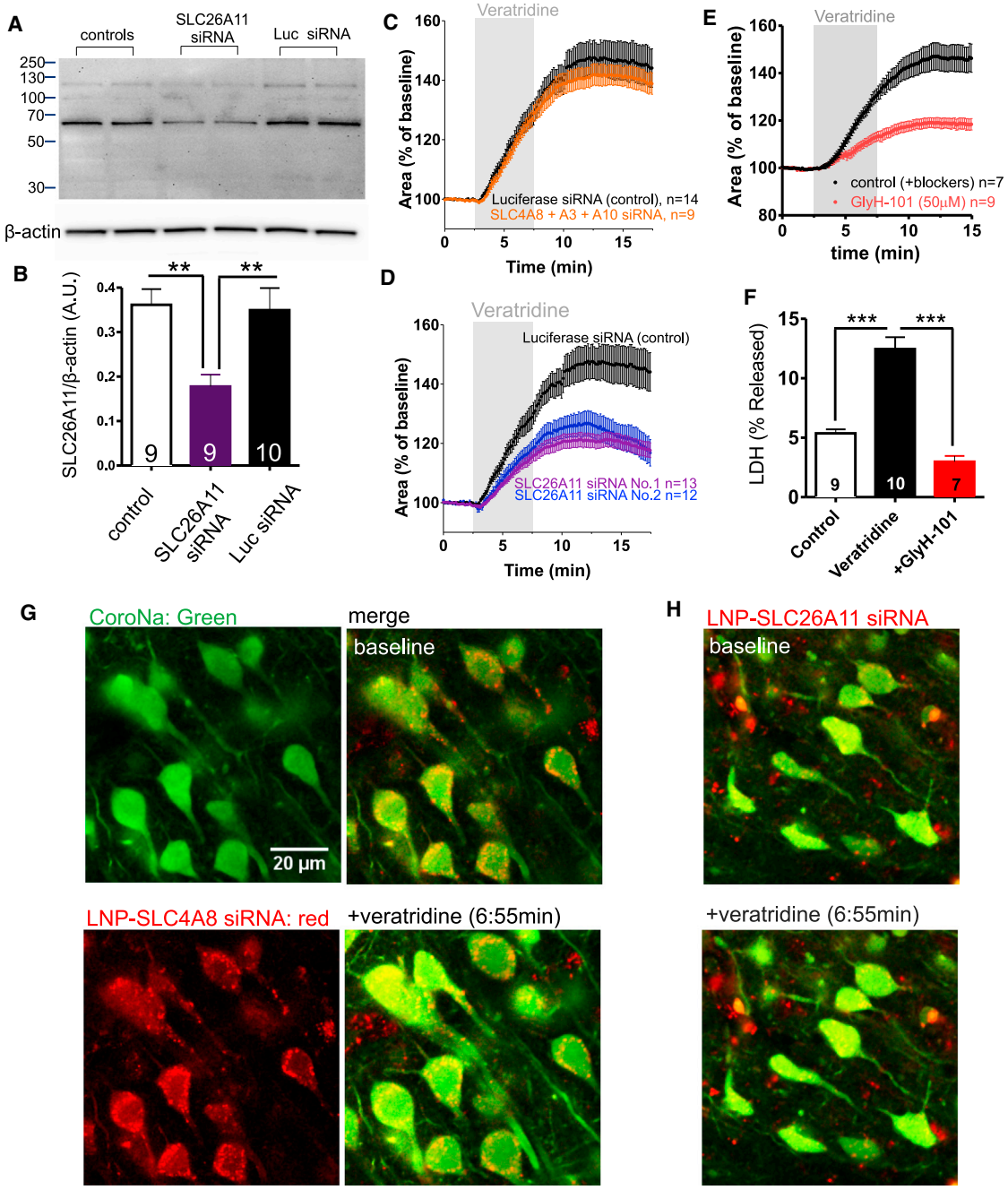

Figure 6. Cl^- Influx via SLC26A11 Causes Cytotoxic Neuronal Edema Following Increased $[Na^+]_i$

(A and B) Cortical brain tissue tested 5 days following in vivo injection of LNP encapsulated siRNAs shows SLC26A11 No.1 siRNA selectively reduced SLC26A11 protein expression compared to β-actin. Controls show luciferase siRNA had no effect on SLC26A11 expression. Columns in (A) represent samples from different rats.

(C) In vivo knockdown of SLC4A3, A8, A10 with LNP-siRNAs results in no significant difference in the magnitude of neuronal swelling compared to a control (luciferase siRNA) in cortical brain slices imaged 5 days following the injection ($p > 0.05$, ANOVA).

(D) Two different siRNA constructs against SLC26A11 result in a significant reduction in the magnitude of veratridine-induced neuronal swelling compared to luciferase siRNA ($p < 0.05$, ANOVA).

(G and H) Example images of cortical neurons transfected with siRNA using lipid nanoparticle delivery shows SLC26A11 knockdown results in protection from veratridine triggered swelling compared to neurons transfected with SLC4A8 siRNA. DiI staining (red) shows cell uptake of LNP-siRNA.

(E and F) SLC26A11 blocker GlyH-101 significantly reduces the magnitude of neuronal swelling induced by increases in $[Na^+]_i$, $p < 0.001$, two-tailed Student's t test (F) and the resulting cell death measured by LDH released, $p < 0.001$, ANOVA.

(legend continued on next page)

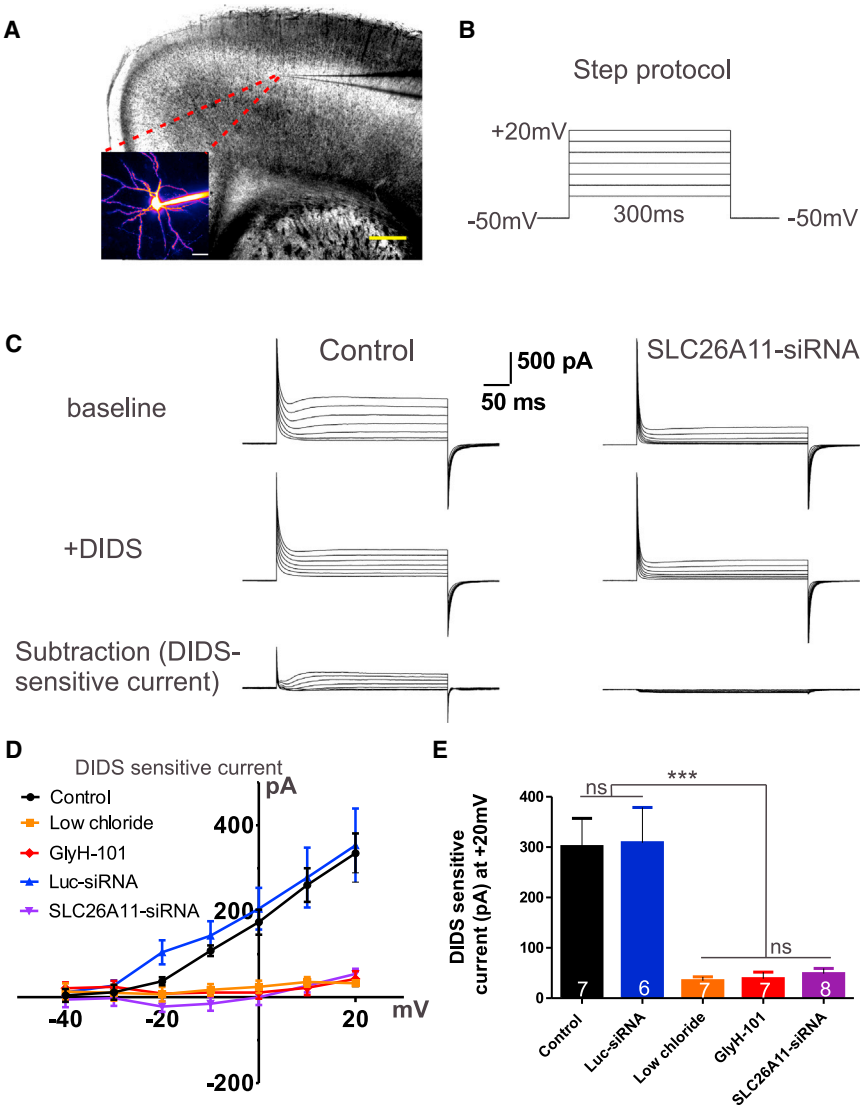

Figure 7. SLC26A11 Gene Product Is Required for Activation of an Outwardly Rectifying Cl^- Channel That Is Activated by Depolarization

(A) Example image of a whole-cell voltage-clamped layer 4 neuron in a coronal brain slice.

(B) Voltage clamp protocol used to depolarize neuron in presence of a cocktail to inhibit known voltage-dependent ion channels.

(C) Left: Top, Example trace of outward current activated by depolarization. Middle, magnitude of current is reduced in DIDS. Bottom, subtraction showing DIDS-sensitive component. Right: SLC26A11 siRNA transfection attenuates DIDS-sensitive outward current.

(D and E) Summarized I/V curves demonstrate that SLC26A11 is required for activation of an outward Cl^- conductance that is activated in depolarized neurons. Low extracellular chloride (10.5 mM), GlyH-101 (50 μM) and SLC26A11 LNP-siRNA all significantly reduce magnitude of DIDS-sensitive current compared to Control and Luc-siRNA transfection. Scale bars in (A): right, 500 μM; left, 25 μM. Error bars represent SEM.

thereby decreased expression of KCC2, leading to decreased recovery of excitotoxic Cl^- loads (Lee et al., 2011). In this study the authors were unable to identify the source of Cl^- influx, but showed that it was independent of NKCC1. If KCC2-mediated Cl^- efflux is indeed compromised following cytotoxic edema, in addition to blocking the influx of Cl^- perhaps enhancing extrusion of Cl^- (Gagnon et al., 2013) would be additionally beneficial.

The identification of SLC26A11 as a significant Cl^- entry pathway during pathological swelling triggered after Na^+ entry suggests new strategies that could be developed toward reducing brain edema. There are numerous different pathways for Na^+ entry that are activated during conditions such as hypoxia, stroke, and TBI. Our observations that cell death is significantly reduced when overall Cl^- entry is prevented suggests that therapeutic strategies to inhibit SLC26A11 dependent Cl^- entry may have widespread benefit toward treating these different conditions.

EXPERIMENTAL PROCEDURES

Imaging

Live-cell imaging (brain slice) was performed with a two-photon laser-scanning microscope (Zeiss LSM510-Axioskop-2; Zeiss, Oberkochen, Germany) with a 40X-W/1.0 numerical aperture objective lens directly coupled to a Chameleon ultra2 laser (Coherent, Santa Clara, CA). CoroNa, SR101 and DiI were excited at 770 nm, and MQAE was excited at 760 nm. The fluorescence from each fluorophore was split using a dichroic mirror at 560 nm, and the signals were each detected with a dedicated photo multiplier tube after passing through an appropriate emission filter (DiI, SR101: 605 nm, 55 nm band pass; CoroNa, MQAE: 525 nm, 50 nm band pass). Transmitted light was simultaneously collected using understage infrared differential interference contrast optics and an additional photo multiplier tube. FLIM methodology is described in detail in the Extended Experimental Procedures.

Data Collection, Analysis, and Statistics

Translational movement was removed using ImageJ software. Fluorescence signals were defined as delta F/F (dF/F) = $[((F_1 - B_1)-(F_0 - B_0))/(F_0 - B_0)]$, where F_1 and F_0 are fluorescence at a given time and the control period mean, respectively. B_1 and B_0 are the corresponding background fluorescence signals. Swelling of individual neurons in cortical slices was analyzed as (%) increase in cross sectional area relative to a mean baseline period. The cross sectional area of the neuron was calculated using the fluorescence boundary

Scale bar in (G) matches scale in (H). Luciferase controls are combined and plotted in both (C and D) and in Figure S5. For statistics on magnitude of swelling, ANOVA was performed comparing results from all siRNA groups (luciferase, SLC4A3, -A8, -A10, -A3+A8+A10, SLC26A11 No.1 and No.2). Only SLC26A11 No.1 and No. 2 were significantly different from luciferase (control) siRNA, $p < 0.05$. Error bars represent SEM. See also Figures S4 and S5 and Movie S5.

of the neuron soma stained with CoroNa. To estimate the tissue volume from the two-dimensional images of hippocampal slices a line was drawn to measure the diameter and the volume was estimated based on the equation for volume of sphere: $(4/3)\pi r^2$.

Experimental values are the mean ± SEM; baseline equals 100%; n is the number of experiments conducted (Imaging data from ≥ 3 individual cells from each experiment were averaged for each n value so that equal weight was given to each experiment and not affected by the number of cells imaged per experiment). Statistical tests were either a two-tailed Student's t test or an ANOVA with a Neumann-Keuls post hoc test for comparison between multiple groups. $p < 0.05$ was accepted as statistically significant (*$p < 0.05$, **$p < 0.01$, ***$p < 0.001$).

More detailed methodology can be found in the Extended Experimental Procedures.

SUPPLEMENTAL INFORMATION

Supplemental Information includes Extended Experimental Procedures, five figures, two tables, and five movies and can be found with this article online at http://dx.doi.org/10.1016/j.cell.2015.03.029.

ACKNOWLEDGMENTS

R.L.R. was supported by a studentship from the Canadian Institutes of Health Research (CIHR), S.L.C. by a fellowship from the BC Epilepsy Society, T.P.S. by an operating grant from the CIHR (#10677) and a Canada Research Chair (CRC) in Biotechnology and Genomics-Neurobiology, P.R.C. by a CIHR Emerging Team Grant: Personalized siRNA-Based Nanomedicines (FRN:111627) and B.A.M. by a CRC in Neuroscience and CIHR operating grants (#8545 and # 115121) and the Fondation Leducq. We thank Dr. Xiling Zhou and Dr. Anne Marie Craig for supplying neuronal cultures and Jeff LeDue for assistance with establishing the FLIM methodology. We thank Kate Campbell for illustrations. The work was also supported by a MIRI grant from Brain Canada, Genome British Columbia, the Michael Smith Foundation for Health Research, and the Koerner Foundation. P.R.C. has greater than 5% ownership of Precision Nanosystems Inc. that makes the systems to formulate the lipid nanoparticles.

Received: December 12, 2014
Revised: February 3, 2015
Accepted: March 12, 2015
Published: April 23, 2015

REFERENCES

Allen, N.J., Rossi, D.J., and Attwell, D. (2004). Sequential release of GABA by exocytosis and reversed uptake leads to neuronal swelling in simulated ischemia of hippocampal slices. J. Neurosci. *24*, 3837–3849.

Alper, S.L., and Sharma, A.K. (2013). The SLC26 gene family of anion transporters and channels. Mol. Aspects Med. *34*, 494–515.

Alvarez-Leefmans, F.J., and Delpire, D. (2009). Physiology and Pathology of Chloride Transporters and Channels in the Nervous System, Vol (London, UK: Elsevier).

Annegers, J.F., Hauser, W.A., Coan, S.P., and Rocca, W.A. (1998). A population-based study of seizures after traumatic brain injuries. N. Engl. J. Med. *338*, 20–24.

Beierlein, M., Gee, K.R., Martin, V.V., and Regehr, W.G. (2004). Presynaptic calcium measurements at physiological temperatures using a new class of dextran-conjugated indicators. J. Neurophysiol. *92*, 591–599.

Berezin, M.Y., and Achilefu, S. (2010). Fluorescence lifetime measurements and biological imaging. Chem. Rev. *110*, 2641–2684.

Blaesse, P., Airaksinen, M.S., Rivera, C., and Kaila, K. (2009). Cation-chloride cotransporters and neuronal function. Neuron *61*, 820–838.

Boron, W.F., Chen, L., and Parker, M.D. (2009). Modular structure of sodium-coupled bicarbonate transporters. J. Exp. Biol. *212*, 1697–1706.

Choi, D.W. (1987). Ionic dependence of glutamate neurotoxicity. J. Neurosci. *7*, 369–379.

Cohen, I., Navarro, V., Clemenceau, S., Baulac, M., and Miles, R. (2002). On the origin of interictal activity in human temporal lobe epilepsy in vitro. Science *298*, 1418–1421.

Donkin, J.J., and Vink, R. (2010). Mechanisms of cerebral edema in traumatic brain injury: therapeutic developments. Curr. Opin. Neurol. *23*, 293–299.

Dreier, J.P. (2011). The role of spreading depression, spreading depolarization and spreading ischemia in neurological disease. Nat. Med. *17*, 439–447.

Ferrini, F., Trang, T., Mattioli, T.A., Laffray, S., Del'Guidice, T., Lorenzo, L.E., Castonguay, A., Doyon, N., Zhang, W., Godin, A.G., et al. (2013). Morphine hyperalgesia gated through microglia-mediated disruption of neuronal Cl^- homeostasis. Nat. Neurosci. *16*, 183–192.

Gagnon, M., Bergeron, M.J., Lavertu, G., Castonguay, A., Tripathy, S., Bonin, R.P., Perez-Sanchez, J., Boudreau, D., Wang, B., Dumas, L., et al. (2013). Chloride extrusion enhancers as novel therapeutics for neurological diseases. Nat. Med. *19*, 1524–1528.

Glykys, J., Dzhala, V., Egawa, K., Balena, T., Saponjian, Y., Kuchibhotla, K.V., Bacskai, B.J., Kahle, K.T., Zeuthen, T., and Staley, K.J. (2014). Local impermeant anions establish the neuronal chloride concentration. Science *343*, 670–675.

Goldberg, M.P., and Choi, D.W. (1993). Combined oxygen and glucose deprivation in cortical cell culture: calcium-dependent and calcium-independent mechanisms of neuronal injury. J. Neurosci. *13*, 3510–3524.

Hasbani, M.J., Hyrc, K.L., Faddis, B.T., Romano, C., and Goldberg, M.P. (1998). Distinct roles for sodium, chloride, and calcium in excitotoxic dendritic injury and recovery. Exp. Neurol. *154*, 241–258.

Hung, C., and Chen, J.W. (2012). Treatment of post-traumatic epilepsy. Curr. Treat. Options Neurol. *14*, 293–306.

Inoue, H., and Okada, Y. (2007). Roles of volume-sensitive chloride channel in excitotoxic neuronal injury. J. Neurosci. *27*, 1445–1455.

Inoue, H., Mori, S., Morishima, S., and Okada, Y. (2005). Volume-sensitive chloride channels in mouse cortical neurons: characterization and role in volume regulation. Eur. J. Neurosci. *21*, 1648–1658.

Jentsch, T.J., Stein, V., Weinreich, F., and Zdebik, A.A. (2002). Molecular structure and physiological function of chloride channels. Physiol. Rev. *82*, 503–568.

Kajta, M., Trotter, A., Lasoń, W., and Beyer, C. (2005). Effect of NMDA on staurosporine-induced activation of caspase-3 and LDH release in mouse neocortical and hippocampal cells. Brain Res. Dev. Brain Res. *160*, 40–52.

Klatzo, I. (1967). Presidental address. Neuropathological aspects of brain edema. J. Neuropathol. Exp. Neurol. *26*, 1–14.

Klatzo, I. (1987). Pathophysiological aspects of brain edema. Acta Neuropathol. *72*, 236–239.

Lee, H.H., Deeb, T.Z., Walker, J.A., Davies, P.A., and Moss, S.J. (2011). NMDA receptor activity downregulates KCC2 resulting in depolarizing GABAA receptor-mediated currents. Nat. Neurosci. *14*, 736–743.

Lee, H.J., Yang, W.S., Park, H.W., Choi, H.S., Kim, S.H., Kim, J.Y., and Choi, J.Y. (2012). Expression of anion exchangers in cultured human endolymphatic sac epithelia. Otology & neurotology *33*, 1664–1671.

Liang, D., Bhatta, S., Gerzanich, V., and Simard, J.M. (2007). Cytotoxic edema: mechanisms of pathological cell swelling. Neurosurg. Focus *22*, E2.

Marmarou, A., Signoretti, S., Fatouros, P.P., Portella, G., Aygok, G.A., and Bullock, M.R. (2006). Predominance of cellular edema in traumatic brain swelling in patients with severe head injuries. J. Neurosurg. *104*, 720–730.

Meier, S.D., Kovalchuk, Y., and Rose, C.R. (2006). Properties of the new fluorescent Na+ indicator CoroNa Green: comparison with SBFI and confocal Na+ imaging. J. Neurosci. Methods *155*, 251–259.

Miles, R., Blaesse, P., Huberfeld, G., Wittner, L., and Kaila, K. (2012). Chloride homeostasis and GABA signaling in temporal lobe epilepsy. In Jasper's Basic Mechanisms of the Epilepsies, J.L. Noebels, M. Avoli, M.A. Rogawski, R.W.

Olsen, and A.V. Delgado-Escueta, eds. (National Center for Biotechnology Information).

Nimmerjahn, A., Kirchhoff, F., Kerr, J.N., and Helmchen, F. (2004). Sulforhodamine 101 as a specific marker of astroglia in the neocortex in vivo. Nat. Methods *1*, 31–37.

Pond, B.B., Berglund, K., Kuner, T., Feng, G., Augustine, G.J., and Schwartz-Bloom, R.D. (2006). The chloride transporter Na(+)-K(+)-Cl- cotransporter isoform-1 contributes to intracellular chloride increases after in vitro ischemia. J. Neurosci. *26*, 1396–1406.

Rahmati, N., Kunzelmann, K., Xu, J., Barone, S., Sirianant, L., De Zeeuw, C.I., and Soleimani, M. (2013). Slc26a11 is prominently expressed in the brain and functions as a chloride channel: expression in Purkinje cells and stimulation of V H^+-ATPase. Pflugers Arch. *465*, 1583–1597.

Romero, M.F., Chen, A.P., Parker, M.D., and Boron, W.F. (2013). The SLC4 family of bicarbonate (HCO_3^-) transporters. Mol. Aspects Med. *34*, 159–182.

Rosenblum, W.I. (2007). Cytotoxic edema: monitoring its magnitude and contribution to brain swelling. J. Neuropathol. Exp. Neurol. *66*, 771–778.

Rothman, S.M. (1985). The neurotoxicity of excitatory amino acids is produced by passive chloride influx. J. Neurosci. *5*, 1483–1489.

Rungta, R.L., Choi, H.B., Lin, P.J., Ko, R.W., Ashby, D., Nair, J., Manoharan, M., Cullis, P.R., and Macvicar, B.A. (2013). Lipid Nanoparticle Delivery of siRNA to Silence Neuronal Gene Expression in the Brain. Mol Ther Nucleic Acids *2*, e136.

Salazar, A.M., Jabbari, B., Vance, S.C., Grafman, J., Amin, D., and Dillon, J.D. (1985). Epilepsy after penetrating head injury. I. Clinical correlates: a report of the Vietnam Head Injury Study. Neurology *35*, 1406–1414.

Smith, R.L., Clayton, G.H., Wilcox, C.L., Escudero, K.W., and Staley, K.J. (1995). Differential expression of an inwardly rectifying chloride conductance in rat brain neurons: a potential mechanism for cell-specific modulation of postsynaptic inhibition. J. Neurosci. *15*, 4057–4067.

Somjen, G.G. (2001). Mechanisms of spreading depression and hypoxic spreading depression-like depolarization. Physiol. Rev. *81*, 1065–1096.

Stewart, A.K., Shmukler, B.E., Vandorpe, D.H., Reimold, F., Heneghan, J.F., Nakakuki, M., Akhavein, A., Ko, S., Ishiguro, H., and Alper, S.L. (2011). SLC26 anion exchangers of guinea pig pancreatic duct: molecular cloning and functional characterization. Am. J. Physiol. Cell Physiol. *301*, C289–C303.

Strichartz, G., Rando, T., and Wang, G.K. (1987). An integrated view of the molecular toxinology of sodium channel gating in excitable cells. Annu. Rev. Neurosci. *10*, 237–267.

Thompson, S.M., Deisz, R.A., and Prince, D.A. (1988). Relative contributions of passive equilibrium and active transport to the distribution of chloride in mammalian cortical neurons. J. Neurophysiol. *60*, 105–124.

Verkman, A.S., and Galietta, L.J. (2009). Chloride channels as drug targets. Nat. Rev. Drug Discov. *8*, 153–171.

Verkman, A.S., Sellers, M.C., Chao, A.C., Leung, T., and Ketcham, R. (1989). Synthesis and characterization of improved chloride-sensitive fluorescent indicators for biological applications. Anal. Biochem. *178*, 355–361.

Vincourt, J.B., Jullien, D., Amalric, F., and Girard, J.P. (2003). Molecular and functional characterization of SLC26A11, a sodium-independent sulfate transporter from high endothelial venules. FASEB J. *17*, 890–892.

Xu, J., Barone, S., Li, H., Holiday, S., Zahedi, K., and Soleimani, M. (2011). Slc26a11, a chloride transporter, localizes with the vacuolar H(+)-ATPase of A-intercalated cells of the kidney. Kidney Int. *80*, 926–937.

Zeuthen, T. (2010). Water-transporting proteins. J. Membr. Biol. *234*, 57–73.

Zhou, N., Gordon, G.R., Feighan, D., and MacVicar, B.A. (2010). Transient swelling, acidification, and mitochondrial depolarization occurs in neurons but not astrocytes during spreading depression. Cereb. Cortex *20*, 2614–2624.

Zhou, N., Rungta, R.L., Malik, A., Han, H., Wu, D.C., and MacVicar, B.A. (2013). Regenerative glutamate release by presynaptic NMDA receptors contributes to spreading depression. J. Cereb. Blood Flow Metab. *33*, 1582–1594.